J. Marine Sci. Appl. (2014) 13:32-40
DOI: 10.1007/s11804-014-1231-4

# Analytical and Experimental Study of Free Vibration of Beams Carrying Multiple Masses and Springs

**Zhuang Wang , Ming Hong*, Junchen Xu and Hongyu Cui**

*School of Naval Architecture Engineering, Dalian University of Technology, Dalian 116024*

**Abstract:**The structures in engineering can be simplified into elastic beams with concentrated masses and elastic spring supports. Studying the law of vibration of the beams can be a help in guiding its design and avoiding resonance.Based on the Laplace transform method, the mode shape functions and the frequency equations of the beams in the typical boundary conditions are derived. A cantilever beam with a lumped mass and a spring is selected to obtain its natural frequencies and mode shape functions. An experiment wasconducted in order to get the modal parameters of the beam based on the NExT-ERA method. By comparing the analytical and experimental results, the effects of the locations of the mass and spring on the modal parameter are discussed. The variation of the natural frequencies was obtained with the changing stiffness coefficient and mass coefficient, respectively. The findings provide a reference for the vibration analysis methods and the lumped parameters layout design of elastic beams used in engineering.

**Keywords:** elastic beams; concentrated masses; springs; natural frequencies; mode shape functions; free vibration; NExT-ERA; modal identification;

**Article ID:** 1671-9433(2014)01-0032-09

## 1 Introduction

Some structures in engineering can be simplified into elastic beams carrying multiple concentrated masses and elastic supports with linear springs. It is very significant to design the parameters and arrange the locations of the lumped masses and springs to obtain excellent vibration characteristics of the beams such as the mast on the ship, the outboard frames in the stern and the outfitting pipelines,*etc*. The designsare mainly related to the effects of the layout of the concentrated stiffness and mass on the vibration system.

There has been extensive research on the vibration analysis of beams carrying concentrated masses or springs at arbitrary locations. Rossit *et al.* (2001) derived the frequency equation of a cantilever beam with a spring–mass system attached to the free end by the analytical method. Banerjee (2012) solved the same problem by a dynamic stiffness approach. Chang (2000) considered the rotational inertia of the lumped mass, and analyzed the free vibration of a simply supported beam with a constant cross-sectional area carrying a concentrated rigid mass at the mid-point of the beam. Low (2003)derived the frequency equation of an Euler-Bernoulli type beam carrying multiple concentrated masses at anarbitrary location by using two methods: frequency determinant and Rayleigh quotient.The results of using the two methods were compared and discussed as well. Then Low (2001) used the Laplace transform method to solve the same problem again. Xia *et al*. (1999)deduced the analytical expressions of the lateral vibration characteristics of a beam with arbitrary lumped masses and elastic spring supports by using the Laplace transform. However, the expressions weretoocomplex so that they were only applicable to the calculation of the beam carrying few masses and springs. Based on the work of Low's, a new analytical expression of the frequency equation and the modal function of the lateral vibration of a beam with lumped masses was derived by means of symbol operation, but the case of springs was neglected (Peng *et al*., 2002). Wu *et al.* (1998) determined the natural frequencies and the corresponding mode shapes of a uniform cantilever beam carrying any number of elastically mounted point masses by means of the analytical and numerical combined method (ANCM). Li *et al.* (2012) obtained the natural frequencies and the modal mode of a flexible beam attaching multiple absorbers by use of the Ritz method. All these research efforts were focused on solving the eigenvalue problems of the beams without considering the influence of concentrated parameters such as the locations of the lumped elements, the stiffness of the springs and the weight of masses. But these studies represent great importance to help with the guidance of the design and to avoid resonance in engineering.

Based on the Laplace transform method, this paper derives the mode shape functions and the frequency equations of the beams carrying multiple lumped masses and elastic spring supports in the typical boundary conditions. A cantilever beam with one concentrated mass and one spring is selected to obtain its natural frequencies and corresponding mode shapes. In order to verify the correctness of the analytical results, an experiment is carried out to get the modal parameters of the beam based on the NExT-ERA method (Jiang *et al.*, 2011). By comparing the analytical and experimental results, the influence of the

**Received date:**2013-08-27.
**Accepted date:**2013-11-01.
**Foundation item:**Supported by the National Natural Science Foundation of China (51109034).
***Corresponding author Email:**mhong@dlut.edu.cn

concentrated parameters like the locations of the lumped elements, the stiffness of the springs and the weight of masses on natural frequenciesare discussed. This data provides a reference for the vibration analysis methods and lumped parameters layout design of the elastic beams in engineering.

## 2Mode shape functions and the frequency equations of the beam

Concerning the uniform elastic beam, the mass and stiffness distribution in the structure is uniformly continuous. The vibration differential equation can be determined through the stress analysis of a micro-section of the beam. And the natural frequencies and mode shape can be obtained by the method of separation of variables. If the beam carries any concentrated masses and concentrated stiffness, its mass and stiffness distribution will no longer be continuous. Therefore, the Dirac delta function ( $\delta$ ) can be introduced to represent the effect of the concentrated masses and stiffness along the beam with various boundary conditions. Due to the existence of the Dirac delta function ( $\delta$ ), the solution of the differential equation becomes complicated.

### 2.1 Mode shape functions

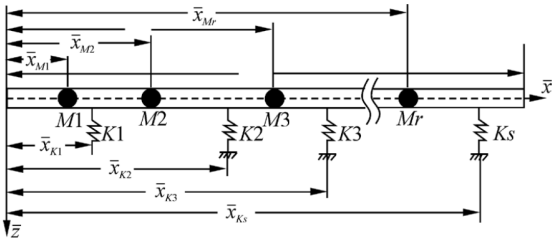


**Fig.1 Elastic beam with lumped masses and springs**

Referring to Fig.1, consider it as a uniform elastic beam with a length of $L$ carrying $r$ concentrated masses and $s$ linear springs. Where $\bar{x}_{Mi}$ and $\bar{x}_{Kj}$ are the spatial coordinates of the $i$th mass and $j$th spring along the beam. The differential equation for the lateral vibration of the beam can be given in the following form:

$$EI\frac{\partial^4 w(\bar{x},t)}{\partial \bar{x}^4}+\rho A\frac{\partial^2 w(\bar{x},t)}{\partial t^2}+\sum_{i=1}^{r}M_i\delta(\bar{x}-\bar{x}_{Mi})\frac{\partial^2 w(\bar{x},t)}{\partial t^2}+\sum_{j=1}^{s}K_j\delta(\bar{x}-\bar{x}_{Kj})w(\bar{x},t)=0 \tag{1}$$

where $E$ is the Young's modulus, $I$ the moment of inertia of the beam's cross-sectional area, $\rho A$ the mass per unit length of the beam, $w(\bar{x},t)$ the transverse deflection of the beam at position $\bar{x}$ and time $t$, $M_i$ the mass of the $i$th lumped mass, $K_j$ the stiffness of the $j$th spring, and $\delta(\cdot)$ the Dirac delta function.

The transverse deflection of the beam may be assumed to be $w(\bar{x},t)=Y(x)\sin\omega t$, where $x=\bar{x}/L$, so the differential Eq. (1) can be written as:

$$\frac{\mathrm{d}^4Y(x)}{\mathrm{d}x^4}-\frac{\rho AL^4\omega^2}{EI}Y(x)=\frac{\omega^2L^3}{EI}\sum_{i=1}^{r}M_iY(x_{Mi})\delta(x-x_{Mi})-\frac{L^3}{EI}\sum_{j=1}^{s}K_jY(x_{Kj})\delta(x-x_{Kj}) \tag{2}$$

By taking the Laplace transform of Eq. (2), we can have:

$$L[Y(x)]=\frac{s^3Y(0)+s^2Y'(0)+sY''(0)+Y'''(0)}{s^4-k^4}+\frac{L^3}{EI(s^4-k^4)}\left[\omega^2\sum_{i=1}^{r}M_iY(x_{Mi})e^{-x_{Mi}s}-\sum_{j=1}^{s}K_jY(x_{Kj})e^{-x_{Kj}s}\right] \tag{3}$$

where $k^4=\dfrac{\rho A}{EI}\omega^2L^4$.

Then taking theinverse Laplace transform of Eq.(3), one obtains:

$$\begin{aligned}Y(x)=&\frac{1}{2}Y(0)(chkx+\cos kx)+\frac{1}{2k}Y'(0)(shkx+\sin kx)+\\&\frac{1}{2k^2}Y''(0)(chkx-\cos kx)+\frac{1}{2k^3}Y'''(0)(shkx-\sin kx)+\\&\frac{L^3\omega^2}{2EIk^3}\sum_{i=1}^{r}M_iY(x_{Mi})[shk(x-x_{Mi})-\sin k(x-x_{Mi})]H(x-x_{Mi})-\\&\frac{L^3}{2EIk^3}\sum_{j=1}^{s}k_jY(x_{Kj})[shk(x-x_{Kj})-\sin k(x-x_{Kj})]H(x-x_{Kj})\end{aligned} \tag{4}$$

where $H(x-x_{Mi})$ and $H(x-x_{Kj})$ are the unit step functions at $x=x_{Mi}$ and $x=x_{Kj}$, respectively.

For convenience, we use the symbol substitution in the forms:

$$\begin{aligned}&S(kx)=\frac{1}{2}(chkx+\cos kx),\ T(kx)=\frac{1}{2k}(shkx+\sin kx)\\&U(kx)\frac{1}{2k^2}(chkx-\cos kx),\ V(kx)=\frac{1}{2k^3}(shkx-\sin kx)\end{aligned} \tag{5}$$

Then they satisfy the following relations:

$$\begin{aligned}&S'(kx)=k^4V(kx),\quad T'(kx)=S(kx)\\&U'(kx)=T(kx),\quad V'(kx)=U(kx)\end{aligned} \tag{6}$$

To substitute Eq.(5) with Eq.(4), one obtains the mode shape function:

$$\begin{aligned}Y(x)=&Y(0)S(kx)+Y'(0)T(kx)+\\&Y''(0)U(kx)+Y'''(0)V(kx)+\\&k^4\sum_{i=1}^{r}\alpha_iY(x_{Mi})V[k(x-x_{Mi})]H(x-x_{Mi})-\\&\sum_{j=1}^{s}\beta_iY(x_{Kj})V[k(x-x_{Kj})]H(x-x_{Kj})\end{aligned} \tag{7}$$

where $\alpha_i = \dfrac{M_i}{\rho AL}$ and $\beta_j = \dfrac{K_j L^3}{EI}$ are the mass coefficient and stiffness coefficient, respectively, which are non-dimensional.

### 2.2 The frequency equation of the beam with a mass and a spring in the middle

To derive the frequency equation, let us assume there are only one concentrated mass and a spring in the middle of the beam, hence in Eq.(1), we have $r=1$, $s=1$, $x_{M1}=1/2$ and $x_{K1}=1/2$.

Consider the clamped-free boundary condition as defined by $Y(0)=Y'(0)=0$, $Y''(1)=Y'''(1)=0$, and substitute $x_{M1}$ and $x_{K1}$ into the derived functions of Eq.(7), respectively, one can obtain:

$$\begin{aligned} Y''(1) &= Y''(0)S(k)+Y'''(0)T(k) \\ &\quad + k^4\alpha_1 Y\left(\frac{1}{2}\right)T\left(\frac{k}{2}\right)-\beta_1 Y\left(\frac{1}{2}\right)T\left(\frac{k}{2}\right) \end{aligned} \tag{8}$$

$$\begin{aligned} Y'''(1) &= Y'(0)k^4V(k)+Y'''(0)S(k) \\ &\quad + k^4\alpha_1 Y\left(\frac{1}{2}\right)S\left(\frac{k}{2}\right)-\beta_1 Y\left(\frac{1}{2}\right)S\left(\frac{k}{2}\right) \end{aligned} \tag{9}$$

The equation $Y\left(\frac{1}{2}\right)=Y''(0)U\left(\frac{k}{2}\right)+Y'''(0)V\left(\frac{k}{2}\right)$ can be obtained from Eq.(7)at $x=\dfrac{1}{2}$, substituting it into Eq.(8) and Eq.(9) yields the expressions:

$$\begin{aligned} Y''(1) &= Y''(0)\left[S(k)+U\left(\frac{k}{2}\right)T\left(\frac{k}{2}\right)\left(\alpha_1k^4-\beta_1\right)\right] \\ &\quad + Y'''(0)\left[T(k)+V\left(\frac{k}{2}\right)T\left(\frac{k}{2}\right)\left(\alpha_1k^4-\beta_1\right)\right] \end{aligned} \tag{10}$$

$$\begin{aligned} Y'''(1) &= Y''(0)\left[k^4V(k)+U\left(\frac{k}{2}\right)S\left(\frac{k}{2}\right)\left(\alpha_1k^4-\beta_1\right)\right] \\ &\quad + Y'''(0)\left[S(L)+V\left(\frac{k}{2}\right)S\left(\frac{k}{2}\right)\left(\alpha_1k^4-\beta_1\right)\right] \end{aligned} \tag{11}$$

The Eq.(10) and Eq.(11) can be written in matrix form:

$$\begin{bmatrix} A_{11} & A_{12} \\ A_{21} & A_{22} \end{bmatrix}\begin{pmatrix} Y''(0) \\ Y'''(0) \end{pmatrix}=0 \tag{12}$$

where $A_{11}=S(k)+U\left(\frac{k}{2}\right)T\left(\frac{k}{2}\right)\left(\alpha_1k^4-\beta_1\right)$,

$A_{12}=T(k)+V\left(\frac{k}{2}\right)T\left(\frac{k}{2}\right)\left(\alpha_1k^4-\beta_1\right)$,

$A_{21}=k^4V(k)+U\left(\frac{k}{2}\right)S\left(\frac{k}{2}\right)\left(\alpha_1k^4-\beta_1\right)$,

$A_{22}=S(k)+V\left(\frac{k}{2}\right)S\left(\frac{k}{2}\right)\left(\alpha_1k^4-\beta_1\right)$,

From the determinant of the matrix in Eq.(12) we can get the transcendental expression of the frequency equation:

$$\begin{aligned} &(\alpha_1k^4-\beta_1)(shk-\sin k+\cos kshk-chk\sin k) \\ &+4k^3(\cos kchk+1)=0 \end{aligned} \tag{13}$$

If the beam is simply supported, the frequency equation can be derived with the following form:

$$2k^3shk\sin k+(\alpha_1k^4-\beta_1)\left(\sin ksh^2\frac{k}{2}-shk\sin^2\frac{k}{2}\right)=0 \tag{14}$$

We can get the frequency equations when the beam is in other boundary conditions by the same approach. It is unnecessary to go into details any more.

### 2.3 The frequency equation of the beam with a mass and a spring at an arbitrary location

In fact, the concentrated mass and spring in the structure can be in any position. So it is necessary to know the variation of the modal parameters of the beam when the masses and springs are in different positions. Consider a cantilever beam, where $\xi_1 L$ and $\xi_2 L$ are the coordinates of the mass and spring in $x$ direction, respectively, as shown in Fig.2.

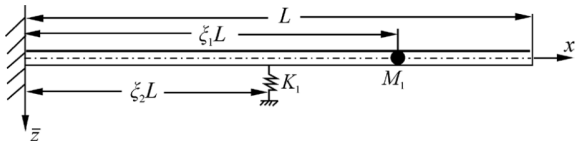


**Fig.2 Beam with lumped masses and lumped springs in random position**

From Eq.(7) and the boundary condition of the cantilever beam, we have the mode shape function:

$$\begin{aligned} Y(x) &= Y''(0)U(kx)+Y'''(0)V(kx) \\ &\quad + k^4\alpha_1 Y(\xi_1)V\left[k(x-\xi_1)\right]H(x-\xi_1) \\ &\quad - \beta_1 Y(\xi_2)V\left[k(x-\xi_2)\right]H(x-\xi_2) \end{aligned} \tag{15}$$

When $\xi_1>\xi_2$, according to the derivation in the previous section one can obtain the determinant of the frequency equation:

$$\begin{vmatrix} B_{11} & B_{12} \\ B_{21} & B_{22} \end{vmatrix}=0 \tag{16}$$

where,

$$\begin{aligned} B_{11} &= S(k)+k^4\alpha_1U(k\xi_1)T\left[k(1-\xi_1)\right] \\ &\quad -\beta_1U(k\xi_2)T\left[k(1-\xi_2)\right] \\ &\quad -k^4\alpha_1\beta_1U(k\xi_2)V\left[k(\xi_1-\xi_2)\right]T\left[k(1-\xi_1)\right] \end{aligned},$$

$$\begin{aligned} B_{12} &= T(k)+k^4\alpha_1V(k\xi_1)T\left[k(1-\xi_1)\right] \\ &\quad -\beta_1V(k\xi_2)T\left[k(1-\xi_2)\right] \\ &\quad -k^4\alpha_1\beta_1V(k\xi_2)V\left[k(\xi_1-\xi_2)\right]T\left[k(1-\xi_1)\right] \end{aligned},$$

$$
\begin{aligned}
B_{21} &= k^4V(k) + k^4\alpha_1U(k\xi_1)S\left[k(1-\xi_1)\right] \\
&\quad - \beta_1U(k\xi_2)S\left[k(1-\xi_2)\right] \\
&\quad - k^4\alpha_1\beta_1U(k\xi_2)V\left[k(\xi_1-\xi_2)\right]S\left[k(1-\xi_1)\right] \\
B_{22} &= S(k + k^4\alpha_1V(k\xi_1)S\left[k(1-\xi_1)\right] \\
&\quad - \beta_1V(k\xi_2)S\left[k(1-\xi_2)\right] \\
&\quad - k^4\alpha_1\beta_1V(k\xi_2)V\left[k(\xi_1-\xi_2)\right]S\left[k(1-\xi_1)\right]
\end{aligned}
$$

Similarly, when $\xi_1 < \xi_2$, we have:

$$
\begin{vmatrix} C_{11} & C_{12} \\ C_{21} & C_{22} \end{vmatrix} = 0 \tag{17}
$$

where,

$$
\begin{aligned}
C_{11} &= S(k) + k^4\alpha_1U(k\xi_1)T\left[k(1-\xi_1)\right] \\
&\quad - \beta_1U(k\xi_2)T\left[k(1-\xi_2)\right] \\
&\quad - k^4\alpha_1\beta_1U(k\xi_1)V\left[k(\xi_2-\xi_1)\right]T\left[k(1-\xi_1)\right] \\
C_{12} &= T(k) + k^4\alpha_1V(k\xi_1)T\left[k(1-\xi_1)\right] \\
&\quad - \beta_1V(k\xi_2)T\left[k(1-\xi_2)\right] \\
&\quad - k^4\alpha_1\beta_1V(k\xi_1)V\left[k(\xi_2-\xi_1)\right]T\left[k(1-\xi_2)\right] \\
C_{21} &= k^4V(k) + k^4\alpha_1U(k\xi_1)S\left[k(1-\xi_1)\right] \\
&\quad - \beta_1U(k\xi_2)S\left[k(1-\xi_2)\right] \\
&\quad - k^4\alpha_1\beta_1U(k\xi_1)V\left[k(\xi_2-\xi_1)\right]S\left[k(1-\xi_2)\right] \\
C_{22} &= S(k) + k^4\alpha_1V(k\xi_1)S\left[k(1-\xi_1)\right] \\
&\quad - \beta_1V(k\xi_2)S\left[k(1-\xi_2)\right] \\
&\quad - k^4\alpha_1\beta_1V(k\xi_1)V\left[k(\xi_2-\xi_1)\right]S\left[k(1-\xi_2)\right]
\end{aligned}
$$

## 3 Modal parameters identification by the natural excitation technique

The natural excitation technique-eigensystem realization algorithm (NExT-ERA) is taken to get the modal parameters of the beam in the experiment in this paper.

### 3.1 Natural excitation technique(NExT)

NExT is a technique used to identify modal parameters under ambient excitation in time domain. This method is based on the assumption that when the system is excited by stationary white noise, the auto- or cross-correlation function of response signals and the impulse response function of the structure have a similar expression.Therefore, the impulse response functions can be replaced by the auto- or cross-correlation function of response signals(James *et al.*, 1995).

### 3.2 Eigensystem realization algorithm (ERA)

The ERA method utilizes the impulse response signals to build the generalized Hankel matrix. The minimal realization of the system is obtained by the singular value decomposition of the Hankel matrix. Based on the minimal order system matrix, one can identify the modal parameters of the system (Xu *et al.*, 2012).

The state space expression of a linear and time discrete system at instant time $t_{k+1}$ is given by:

$$
\begin{cases} \boldsymbol{x}(k+1) = \boldsymbol{A}\boldsymbol{x}(k) + \boldsymbol{B}\boldsymbol{u}(k) \\ \boldsymbol{y}(k) = \boldsymbol{C}\boldsymbol{x}(k) + \boldsymbol{D}\boldsymbol{u}(k) \end{cases} \tag{18}
$$

where $k$ represents the discrete time, $\boldsymbol{x}(k)$ is the state vector, $\boldsymbol{u}(k) = \boldsymbol{u}(k\Delta t)$ and $\boldsymbol{y}(k) = \boldsymbol{y}(k\Delta t)$ are input and output vectors, respectively. $\boldsymbol{A}$, $\boldsymbol{B}$ and $\boldsymbol{C}$ are the system, input and output matrices, respectively.

Assuming that the number of impulse inputs on the system is *S*,and the number of output sensors is *M*,the mathematical model of ERA can be described as:

$$
\begin{aligned}
&\boldsymbol{h}(0) = \boldsymbol{y}(0) = \boldsymbol{D}, \quad \boldsymbol{h}(1) = \boldsymbol{y}(1) = \boldsymbol{CB}, \\
&\boldsymbol{h}(2) = \boldsymbol{y}(2) = \boldsymbol{CAB}, \quad \cdots, \quad \boldsymbol{h}(k) = \boldsymbol{y}(k) = \boldsymbol{CA}^{k-1}\boldsymbol{B}
\end{aligned} \tag{19}
$$

where $\boldsymbol{h}(k)$ is the impulse response matrix.Forming the Hankel matrix:

$$
\boldsymbol{H}(k-1) = \begin{bmatrix} \boldsymbol{h}(k) & \boldsymbol{h}(k+1) & \cdots & \boldsymbol{h}(k+\beta-1) \\ \boldsymbol{h}(k+1) & \boldsymbol{h}(k+2) & \cdots & \boldsymbol{h}(k+\beta) \\ \vdots & \vdots & \ddots & \vdots \\ \boldsymbol{h}(k+\alpha-1) & \boldsymbol{h}(k+\alpha) & \cdots & \boldsymbol{h}(k+\alpha+\beta-2) \end{bmatrix}_{\alpha M \times \beta S} \tag{20}
$$

where $\alpha$ and $\beta$ are arbitrary integers.When $k=1$, one obtains the singular value decomposition (SVD) of Hankel matrix $\boldsymbol{H}(0)$:

$$
\boldsymbol{H}(0) = \boldsymbol{U}\boldsymbol{\Sigma}\boldsymbol{V}^{\mathrm{T}} \tag{21}
$$

where $\boldsymbol{\Sigma} = \begin{bmatrix} \boldsymbol{\Sigma}_n & \boldsymbol{0} \\ \boldsymbol{0} & \boldsymbol{0} \end{bmatrix}$, $\boldsymbol{\Sigma}_n = \mathrm{diag}\left[\sigma_1, \sigma_2, \cdots \sigma_n\right]$, $n$ is an even number which represents the system order. Hence, define $\boldsymbol{U}_n$ and $\boldsymbol{V}_n$ to be the first $n$ column of orthonormal matrices $\boldsymbol{U}$ and $\boldsymbol{V}$, respectively. When $k=2$, in a similar way one can obtain:

$$
\boldsymbol{H}(1) = \boldsymbol{PAQ} = \boldsymbol{U}_n\boldsymbol{\Sigma}_n^{1/2}\boldsymbol{A}\boldsymbol{\Sigma}_n^{1/2}\boldsymbol{V}_n^{\mathrm{T}} \tag{22}
$$

Defining $\boldsymbol{E}_M^{\mathrm{T}} = \left[\boldsymbol{I}_M \quad \boldsymbol{0}_M \quad \cdots \quad \boldsymbol{0}_M\right]_{M \times \alpha M}$ and $\boldsymbol{E}_S^{\mathrm{T}} = \left[\boldsymbol{I}_S \quad \boldsymbol{0}_S \quad \cdots \quad \boldsymbol{0}_S\right]_{S \times \beta S}$. The minimal realization of the system is achieved:

$$
\begin{aligned}
\boldsymbol{A} &= \boldsymbol{\Sigma}^{-1/2}\boldsymbol{U}^T\boldsymbol{H}(1)\boldsymbol{V}\boldsymbol{\Sigma}^{-1/2} \\
\boldsymbol{B} &= \boldsymbol{\Sigma}^{1/2}\boldsymbol{V}^{\mathrm{T}}\boldsymbol{E}_S \\
\boldsymbol{C} &= \boldsymbol{E}_M^{\mathrm{T}}\boldsymbol{U}\boldsymbol{\Sigma}_n^{1/2}
\end{aligned} \tag{23}
$$

The eigenvalue decomposition (EVD) of the discrete time system matrix $\boldsymbol{A}$ can be written as:

$$
\boldsymbol{A} = \boldsymbol{\psi}^{-1}\boldsymbol{Z}\boldsymbol{\psi} \tag{24}
$$

where $\boldsymbol{Z}$ and $\boldsymbol{\psi}$ are the eigenvalue matrix and eigenvector matrix of $\boldsymbol{A}$, respectively.

The eigenvectors of the continuous-time system matrix $\boldsymbol{A}_C$ are the same as those of $\boldsymbol{A}$. And the eigenvalue of them satisfies the relationship:

$$\lambda_i = \frac{1}{\Delta t}\ln z_i \quad (i = 1,2,\cdots,2N) \tag{25}$$

where $z_i$ is the diagonal element of the eigenvalue matrix $\boldsymbol{Z}$, and $\lambda_i$ the eigenvalue of $\boldsymbol{A}_c$.

According to the modal theory, the modal frequency, the modal damping ratio and the modal shape matrix are in the following forms:

$$\begin{aligned} \omega_i &= \sqrt{\mathrm{Re}(\lambda_i)^2 + \mathrm{Im}(\lambda_i)^2} \\ \zeta_i &= \frac{\mathrm{Re}(\lambda_i)}{\sqrt{\mathrm{Re}(\lambda_i)^2 + \mathrm{Im}(\lambda_i)^2}} \\ \boldsymbol{\Psi}' &= \boldsymbol{C}\boldsymbol{\psi} \end{aligned} \tag{26}$$

## 4 Comparisons of numerical and experimental results and discussions

### 4.1 Effects of the mass coefficient and stiffness coefficient on natural frequencies

In order to study the influences of the size of mass and the stiffness of the spring on natural frequency, using the above theory, numerical results are obtained from a cantilever beam with a lumped mass at the tip and a spring in the middle, as shown in Fig.4. The mass coefficient $\alpha$ and stiffness coefficient $\beta$ have three different values, respectively. To make a comparison between the analytical and experimental results, the material parameters of the beam are all given the same values as that in the experiment, as shown in Table 1 and Table 2. The first four natural frequencies $\omega_{an}$ computed analytically for different values of $\alpha$ and $\beta$ are shown in Tables 3 - 5.

An experiment is carried out to identify the modal parameters of the cantilever beam based on the above NExT-ERA method as shown in Fig.3 and Fig.4. The material properties of the beam are shown in Table 1. The three different values of mass and stiffness used are shown in Table 2. In the experiment, the mass and the spring can be fixed in the beam at arbitrary positions. A white noise excitation is applied to the beam near the clamped end. The response of acceleration can be obtained by the sensors. The first four natural frequencies $\omega_{ex}$ identified in the experiment for different values of $\alpha$ and $\beta$ are also listed in Tables 3 - 5.

In addition, in order to verify the correctness of the analytical and experimental results further, the frequencies $\omega_{\mathrm{FEM}}$ obtained by ANSYS are also shown in the Tables.

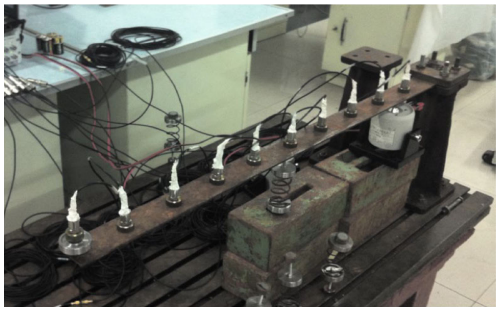

**Fig.3 Testing ground**

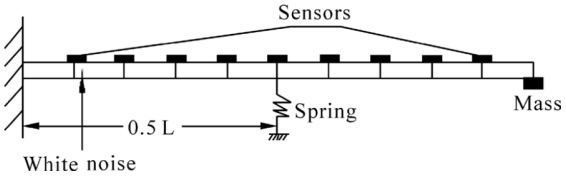


**Fig.4 The experimental model**

**Table 1 Material properties of the beam**

| Material properties | values |
|---|---|
| Young's modulus $E$ / GPa | 210 |
| Density $\rho$ /(kg·m$^{-3}$) | 7850 |
| Poisson ratio $\mu$ | 0.3 |
| Length $L$ / m $L$ ) | 0.85 |
| Cross-sectional area A / m$^2$ | 3.0E−4 |
| Moment of inertia $I$ / (m$^4$) | 9.0E−10 |

**Table 2 Properties of the masses and springs**

| springs | | masses | |
|---|---|---|---|
| $K$ (/N·m$^{-1}$) | $\beta=\frac{KL^3}{EI}$ | $M$ / kg | $\alpha=\frac{M}{\rho AL}$ |
| 1.135E3 | 3.6881 | 0.1515 | 0.07568 |
| 3.920E3 | 12.7376 | 0.2470 | 0.12339 |
| 6.697E3 | 21.7612 | 0.3705 | 0.18509 |

From Table 3, Table 4 and Table 5, it can be seen that the analytical results agree well with the experimental ones. And the numerical ones obtained by ANSYS further prove the correctness of the analytical approach in this paper.

Referring to the resultsshown in the Tabs, it is clear that when the positions of the mass and spring are fixed and the value of $\alpha$ is kept constant, the natural frequencies increase as the value of $\beta$ increases. If the value of $\beta$ is kept constant, the natural frequencies decrease as the value of $\alpha$ increases. As we know, according to the single degree of freedom system (SDOF), its natural frequency is proportional to the stiffness of the system, and inversely proportional to the mass. And the variations of the natural frequencies of the beam also comply with this rule.

It should be noted that the experimental results of the natural frequencies will be a little less than the analytical ones due to the effect of the mass of the sensors.

**Table 3 The first four natural frequencies when $\alpha$=0.07568 , $\beta$ has different valuesHz**

| $n$ | $\beta$=3.6881 | | | $\beta$=12.7376 | | | $\beta$=21.7612 | | |
|---|---|---|---|---|---|---|---|---|---|
| | $\omega_{an}$ | $\omega_{ex}$ | $\omega_{FEM}$ | $\omega_{an}$ | $\omega_{ex}$ | $\omega_{FEM}$ | $\omega_{an}$ | $\omega_{ex}$ | $\omega_{FEM}$ |
| 1 | 6.429 | 5.938 | 6.413 | 7.267 | 7.031 | 7.258 | 7.933 | 7.813 | 7.918 |
| 2 | 39.431 | 34.688 | 39.284 | 40.318 | 35.156 | 40.179 | 41.196 | 36.563 | 41.059 |
| 3 | 111.212 | 105.531 | 110.558 | 111.241 | 101.250 | 110.572 | 111.241 | 102.031 | 110.585 |
| 4 | 220.897 | 193.594 | 218．898 | 220.897 | 194.531 | 219.046 | 221.314 | 195.156 | 219.193 |

**Table 4 The first four natural frequencies when $\alpha$=0.12339 , $\beta$ has different valuesHz**

| $n$ | $\beta$=3.6881 | | | $\beta$=12.7376 | | | $\beta$=21.7612 | | |
|---|---|---|---|---|---|---|---|---|---|
| | $\omega_{an}$ | $\omega_{ex}$ | $\omega_{FEM}$ | $\omega_{an}$ | $\omega_{ex}$ | $\omega_{FEM}$ | $\omega_{an}$ | $\omega_{ex}$ | $\omega_{FEM}$ |
| 1 | 6.023 | 5.469 | 6.017 | 6.761 | 6.563 | 6.756 | 7.358 | 7.188 | 7.358 |
| 2 | 37.893 | 33.281 | 37.789 | 38.833 | 33.750 | 38.716 | 39.749 | 35.352 | 39.627 |
| 3 | 108.327 | 102.540 | 107.808 | 108.356 | 98.594 | 107.828 | 108.386 | 99.531 | 107.849 |
| 4 | 216.741 | 193.112 | 215.293 | 217.154 | 193.563 | 215.441 | 217.237 | 194.969 | 215.598 |

**Table 5 The first four natural frequencies when $\alpha$=0.18509 , $\beta$ has different valuesHz**

| $n$ | $\beta$=3.6881 | | | $\beta$=12.7376 | | | $\beta$=21.7612 | | |
|---|---|---|---|---|---|---|---|---|---|
| | $\omega_{an}$ | $\omega_{ex}$ | $\omega_{FEM}$ | $\omega_{an}$ | $\omega_{ex}$ | $\omega_{FEM}$ | $\omega_{an}$ | $\omega_{ex}$ | $\omega_{FEM}$ |
| 1 | 5.557 | 5.000 | 5.555 | 6.239 | 6.094 | 6.237 | 6.783 | 6.719 | 6.781 |
| 2 | 36.573 | 32.300 | 36.492 | 37.548 | 32.969 | 37.454 | 38.484 | 34.063 | 38.391 |
| 3 | 106.087 | 100.200 | 105.669 | 106.116 | 96.250 | 105.696 | 106.145 | 97.656 | 105.724 |
| 4 | 213.855 | 192.200 | 212.694 | 214.266 | 190.156 | 212.840 | 214.266 | 191.250 | 212.987 |

From Eq.(15), with the condition of $r$=1, $s$=1, $x_{M1}=1$ and $x_{K1}=1/2$ , the mode shape function can be written as:

$$Y(x)=Y''(0)\left[U(kx)-\beta_1 U\left(\frac{k}{2}\right)V\left(kx-\frac{k}{2}\right)H\left(x-\frac{1}{2}\right)\right] + Y'''(0)\left[V(kx)-\beta_1 V\left(\frac{k}{2}\right)V\left(kx-\frac{k}{2}\right)H\left(x-\frac{1}{2}\right)\right] \quad (27)$$

where the $Y''(0)$ and $Y'''(0)$ can be obtained from Eq.(12).

When $\alpha$=0.12339 and $\beta$=21.7612 , one can have the first four mode shapes as shown in Fig.5. And the identified ones by experiment are shown in Fig.6. It is clear that the results agree well with each other.

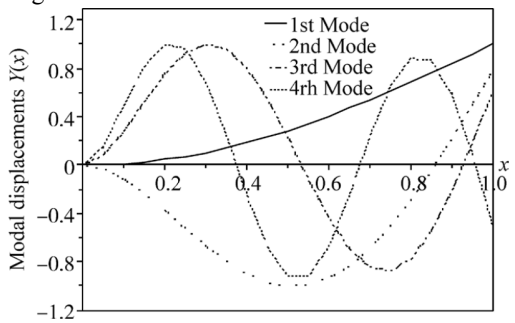


**Fig.5 The analytical first four mode shapes**

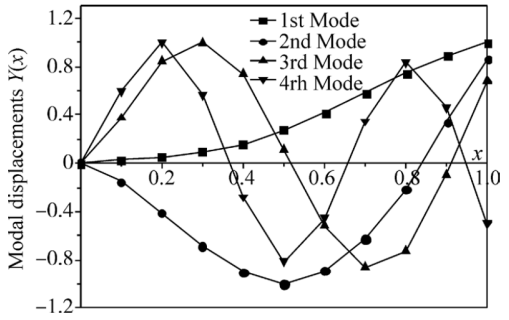


**Fig.6 The first four mode shapes obtained from experiment**

### 4.2 Effects of the locations of the mass and spring on natural frequencies

To study the effects of the locations of the spring on natural frequencies, we have the beam with a mass fixed in the end and the spring in nine different positions along the beam. This means that we have $\xi_1$=1 and $\xi_2=0.1, 0.2, \ldots, 0.9$ in the Eq.(16) and Eq.(17). The mass and spring coefficient are $\alpha_1$=0.12339 and $\beta_1$=21.7612 , respectively. The first four natural frequencies fo r different values of $\beta$ are computed analytically. Moreover, the results are also obtained by experiment so as to be compared with the analytical ones.

For presentational purposes, the curves are plotted which

indicates the variation of each order of natural frequency $\omega_i$ with the spring moving from one end to the other as shown in Fig.7.

Similarly, when $\xi_2$=1 and $\xi_1 = 0.1, 0.2, \ldots, 0.9$ in the Eq.(16) and Eq.(17), the changing of each order natural frequency $\omega_i$ with the mass moving from the clamped end to another are also obtained as shown in Fig.8.

Referring to the curves illustrated inFig.7 and Fig.8, it is clear that the analytical results agree well with the experimental ones. And it has been found that when the spring moves from the clamped end to the free end along the beam, the variation trends of $\omega_i$ in both sets of results are particularly regular. When comparing the curves with the mode shapes in Fig.5 or Fig.6, it is seen that the $\omega_1 - \xi_2$ curve is similar to the first order mode shape and the $\omega_2 - \xi_2$ curve is similar to the second order mode shape. Furthermore, the $\omega_3 - \xi_2$ curve and $\omega_4 - \xi_2$ curve comply with the same laws.

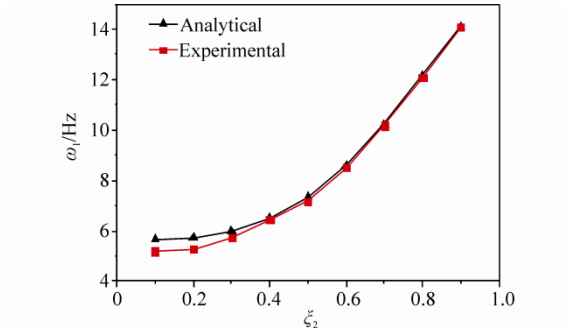


(a) variation of $\omega_1$ with $\xi_2$

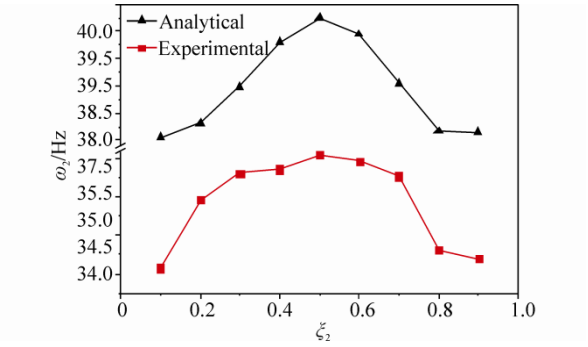


(b) variation of $\omega_2$ with $\xi_2$

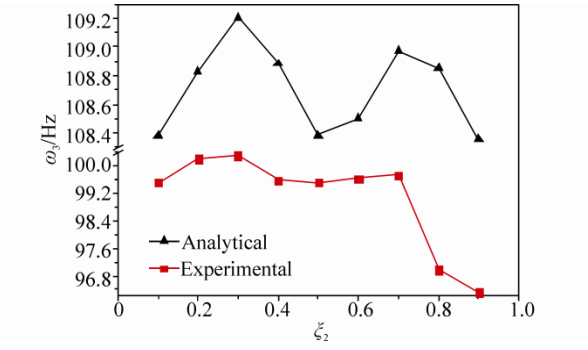


(c) variation of $\omega_3$ with $\xi_2$

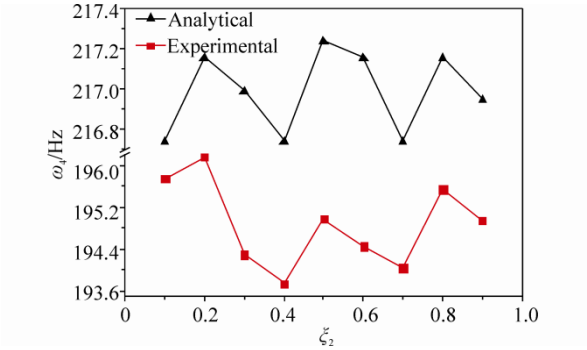


(d) variation of $\omega_4$ with $\xi_2$

**Fig.7 The variation of the first four natural frequencies with the spring in different positions**

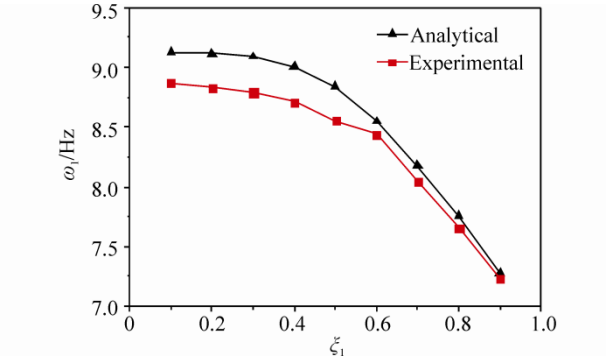


(a) variation of $\omega_1$ with $\xi_1$

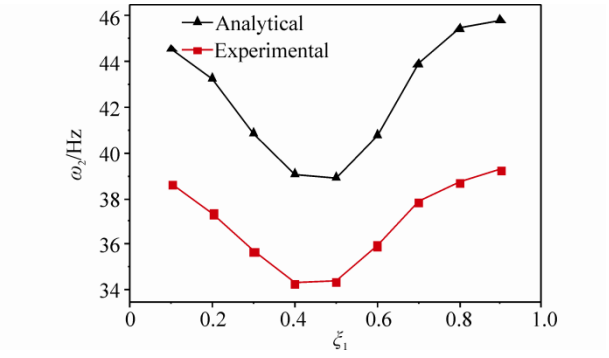


(b) variation of $\omega_2$ with $\xi_1$

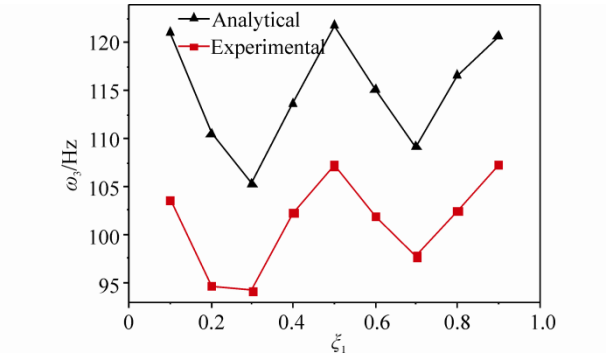


(c) variation of $\omega_3$ with $\xi_1$

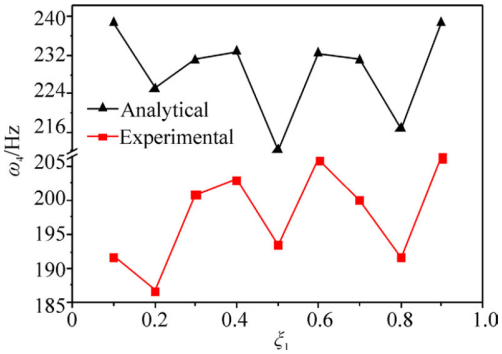


(d) variation of $\omega_4$ with $\xi_1$

**Fig.8 The variation of the first four natural frequencies with the mass in different positions**

These change laws of $\omega_i$ are not coincidental but predictable. To the first order mode shape of the cantilever beam, its nodal displacement is gradually increasing from the fixed end to the free end. As we know, to a multiple degree of freedom system(MDOF),the *i*th natural frequency is $\omega_i=\sqrt{K_i/M_i}$, where $K_i$ is the *i*th modal stiffness, $M_i$ is the *i*th modal mass. When the spring moves from the fixed end to the free end, the $K_i$ of the beam is changing. Take the first mode of the beam shown in Fig.9(a) and Fig.9(b) as an example. In the condition of (b), the spring located at the position having a larger nodal displacement, leads to the spring having a stronger constraint to the beam than that of in the condition of (a). So the first modal stiffness $K_{1a}$ of the beam in condition (a) is smaller than the ones at $K_{1b}$ in condition (b). According to the equation above, the first order natural frequency $\omega_1$ in condition (a) is smaller than the ones in condition (b). The first order modal stiffness $K_1$ of the beam increases gradually when the spring moves from the fixed end to the free end. So the first order natural frequency $\omega_1$ is increasing as the $\xi_2$ is changing. For the second order mode shape, the peak displacement is in the middle of the beam, so the constraint on the beam first increases and then decreases which leads to the result that the second order modal stiffness $K_2$ increases first and then decreases. As a result, the second order natural frequency $\omega_2$ increases firstly and then decreases,so these are the variations of the third and fourth order natural frequencies.

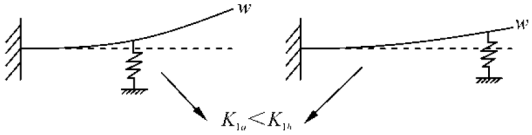


(a) Spring is in the middle (b) Spring is near the free end

**Fig.9 The modal stiffness when the spring is in different positions**

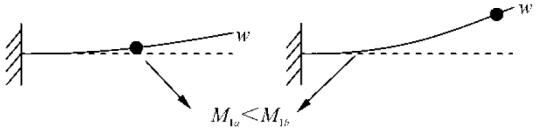


(a)Mass is in the middle (b) Mass is near the free end

**Fig.10 The modal mass when the mass is in different positions**

However, when the mass moves along the beam, the changing trends of the frequencies are just the opposite to the ones moving the spring. As shown in Fig.10(a) and Fig.10(b), the first order modal mass $M_{1a}$ of the beam in condition (a) is smaller than $M_{1b}$ in condition (b), so the first natural frequency $\omega_1$ in condition (a) is bigger than the ones in condition (b). With an analogy of this, the mass moving from the fixed end to the free end increases the first order modal mass $M_1$, which decreases the first order natural frequency $\omega_1$. For the second mode, the second order modal mass $M_2$ increases first and then decreases. So the second order natural frequency $\omega_2$ first decreases and then increases.

## 5 Conclusion

The structures in engineering can be simplified into elastic beams with concentrated masses and lumped elastic supports. Studying the law of vibration of these beams can help guide their design and avoid resonance. In this paper, an analytical approach and a modal identification experiment were taken at the same time to obtain the mode shape functions and frequency equations of the beams carrying multiple concentrated masses and springs. And the modal analysis experiment was carried out by use of the NExT-ERA method to identify the modal parameters of the beam.

The variation of the natural frequencies of the beam is discussed by comparing the analytical results with the experimental results. The two sets of results are consistent with each other. This proves the correctness of the analytical approach and the validity of the NExT-ERA method. Concerning the cantilever beam with one mass and a single spring, the effects of the mass coefficient and stiffness coefficient on the natural frequencies is similar to those of the single degree of freedom system. The effects of the locations of the mass and springs on the natural frequencies are related to the orders of the mode shapes.

## References

Banerjee JR (2012). Free vibration of beams carrying spring-mass systems: a dynamic stiffness approach. *Computers and Structures*, **21**(26), 104-105.

Chang CH (2000). Free vibration of a simply supported beam carrying A rigid mass at the middle. *Journal of Sound and Vibration*, **237**, 733-744.

Gurgoze M (1996). On the eigenfrequencies of a cantilever beam with attached tip mass and a spring-mass system. *Journal of Sound and Vibration*, **190**, 149-162.

Jiang DZ, Hong M, Zhou L (2011). Study on operational modal parameters identification of ship structures. *Journal of Ship Mechanics*, **15**(3), 313-324.

James GH, Carne JPL (1995). The natural excitation technique (NExT) for modal parameter extraction from operating Structures. *Journal of Analytical and Experimental Modal Analysis*, **10**(4), 260-277.

Li J, Liu CS, Li F (2012). Modal analysis of a flexible beam attaching multiple absorbers. *Applied Mechanics and Materials*, **226-228**, 154-157.

Lin HY, Tsai YC (2007). Free vibration analysis of a uniform multi-span beam carrying multiple spring–mass systems. *Journal of Sound and Vibration*, **302**, 442-456.

Low KH (2003). Frequencies of beams carrying multiple masses: Rayleigh estimation versus eigen-analysis solutions. *Journal of Sound and Vibration*, **268**, 843-853.

Low KH (2001). On the methods to derive frequency equations of beams carrying multiple masses. *International Journal of Mechanical Sciences*, **43**, 871-881.

Mohanty P, Rixen DJ (2006). Modified ERA method for operational modal analysis in the presence of harmonic excitations. *Mechanical Systems and Signal Processing*, **20**, 114-130.

Peng X, Peng F (2002). New analytical expressions of lateral vibration characteristics of a beam with lumped masses. *Journal of Hunan University*, **29**, 44-48.(in Chinese)

Rossit CA, Laura PAA (2001). Free vibrations of a cantilever beam with a spring–mass system attached to the free end. *Ocean Engineering*, **28**, 933-939.

Wu JS, Chou HM (1998). Free vibration analysis of a cantilever beam carrying any number of elastically mounted point masses with the analytical and numerical combined method. *Journal of Sound and Vibration*, **213**, 317-332.

Wu JS, Chou HM (1999). A new approach for determining the natural frequencies and mode shapes of a uniform beam carrying any number of sprung masses. *Journal of Sound and Vibration*, **200**, 451-468.

Xia J, Zhu MC, Ma DY (1999). Analysis of lateral natural vibration of beams with lumped masses and elastic supports. *Journal of Southwest Institute of Technology*, **14**, 1-4.(in Chinese)

Xu JC，Hong M, Cui HY (2012). The Contrast Experimental Study on Operational Modal Analysis of Ship Structural Model. *Applied Mechanics and Materials*, **226-228**, 241-246.

## Author biography

**Ming Hong** is a professor at the School of Naval Architecture, DalianUniversityof Technology. His research interests include ship vibration analysis, control and experiment, acoustic transmission in multi-media, *etc*. He is a senior member of the China Shipbuilding Institute and a member of the Ship Mechanics Committee.